Structure
Short Article

Functional Diversity of Tandem Substrate-Binding Domains in ABC Transporters from Pathogenic Bacteria

Faizah Fulyani,[1,2] Gea K. Schuurman-Wolters,[1,2] Andreja Vujičić Žagar,[1,2] Albert Guskov,[1] Dirk-Jan Slotboom,[1] and Bert Poolman[1,*]
[1]Department of Biochemistry, Groningen Biomolecular Sciences and Biotechnology Institute, Netherlands Proteomics Centre and Zernike Institute for Advanced Materials, University of Groningen, Nijenborgh 4, 9747 AG Groningen, the Netherlands
[2]These authors contributed equally to this work
*Correspondence: b.poolman@rug.nl
http://dx.doi.org/10.1016/j.str.2013.07.020

SUMMARY

The ATP-binding cassette (ABC) transporter GlnPQ is an essential uptake system for amino acids in gram-positive pathogens and related nonpathogenic bacteria. The transporter has tandem substrate-binding domains (SBDs) fused to each transmembrane domain, giving rise to four SBDs per functional transporter complex. We have determined the crystal structures and ligand-binding properties of the SBDs of GlnPQ from *Enterococcus faecalis*, *Streptococcus pneumoniae*, and *Lactococcus lactis*. The tandem SBDs differ in substrate specificity and affinity, allowing cells to efficiently accumulate different amino acids via a single ABC transporter. The combined structural, functional, and thermodynamic analysis revealed the roles of individual residues in determining the substrate affinity. We succeeded in converting a low-affinity SBD into a high-affinity receptor and vice versa. Our data indicate that a small number of residues that reside in the binding pocket constitute the major affinity determinants of the SBDs.

INTRODUCTION

ATP-binding cassette (ABC) transporters have been subdivided into exporters and type I, II, and III importers based on the structures of their integral membrane domains (Erkens et al., 2012; Rees et al., 2009). Exporters mediate transport of molecules from the cytoplasm to the external medium or organelle lumen. They bind their ligands directly within the transmembrane domain (TMD), without the need for auxiliary proteins. Type I and II importers capture their ligands via soluble substrate-binding proteins (SBP). Type III importers, also known as ECF-type ABC transporters (Rodionov et al., 2009), capture a substrate via membrane-embedded S-components (Erkens et al., 2011), associated with the energy-coupling factor (ECF). Upon substrate binding, the SBPs of type I and II importers change conformation from open to closed and, subsequently, dock onto the TMD. Generally, both type I and II importers follow a so-called two state alternating access model in which the transporter adopts either an outward- or inward-facing conformation, thus allowing substrate to be transferred from the external medium to the cytoplasm. The mechanism of transport of type I and II importers is quite different. In type I, as exemplified by the maltose transporter MalE-MalFGK$_2$ from *Escherichia coli* (Oldham and Chen, 2011; Orelle et al., 2008), liganded MalE interacts with low affinity to inward-facing MalFG, which then triggers ATP binding and closure of the nucleotide-binding domains (NBDs) and the transfer of substrate from the SBP to the TMD (Böhm et al., 2013; Davidson et al., 2008). Subsequent hydrolysis of ATP and release of inorganic phosphate (P_i) and ADP completes the translocation cycle and resets the system to the ground state. In an alternative model, binding of ATP triggers the outward-facing conformation of MalFG to which unliganded MalE binds with high affinity (Bao and Duong, 2013). Binding of maltose to MalE-MalFGK$_2$ would then initiate substrate translocation. In type II importers (e.g., the vitamin B12 transporter, BtuF-BtuCD), the transport is initiated by docking of liganded ButF to the outward-facing conformation of the transporter (Korkhov et al., 2012; Rice et al., 2013; Joseph et al., 2011). Binding of ATP closes the NBDs as well as the periplasmic and cytoplasmic gates, and the substrate gets trapped in a translocation cavity (“occluded state”). Subsequent ATP hydrolysis opens the cytoplasmic gate and releases the substrate on the *trans* side of the membrane (Korkhov et al., 2012).

Soluble SBPs were first discovered in the periplasm of the gram-negative bacterium *E. coli*, thus they are often referred to as periplasmic binding proteins (Berger and Heppel, 1974). In microorganisms lacking an outer membrane and periplasm, i.e., gram-positive bacteria and Archaea, SBPs are exposed on the cell surface. Typically, they are attached to the cytoplasmic membrane via either a lipid anchor or a membrane-embedded peptide (the latter has only been observed in Archaea) or they are fused to the TMDs, resulting in two substrate-binding domains (SBDs) per functional complex. In some cases, two or even three SBDs are fused together and linked to the TMDs, generating four or six extracytoplasmic substrate-binding sites. Transporters with SBDs fused to the TMDs occasionally are also present in gram-negative bacteria, but less frequently than in gram-positive bacteria (van der Heide and Poolman, 2002). The linkage of SBDs to the membrane and fusing of (multiple) SBDs to the TMD increase the effective concentration of the

substrate-binding sites near the translocator. SBDs are not only associated with ABC transporters, but are also present in ion-linked transporters, ion channels, G protein-coupled receptors, and two-component regulatory systems, and they are found in prokaryotes and eukaryotes (Berntsson et al., 2010). Despite their importance in biology and the availability of many crystal structures, the mechanism of ligand binding is still poorly understood, thus it is difficult to predict ligand specificity from protein structure and to rationally design drugs. What is needed is a better description of the functional and thermodynamic properties of SBDs in relation to structural information.

Here, we focus on the functional and structural analysis of type I ABC importers with two SBDs fused in tandem (termed as SBD1 and SBD2 for the individual domains and SBD12 for the tandem), which are prominent in gram-positive pathogenic bacteria. These transporters are among the most complex systems of the ABC superfamily, and the functional role of dual SBDs is poorly understood. We reveal the specificity determinants of the SBDs by analysis of the orthologous GlnPQ importers from the nonpathogenic *Lactococcus lactis* and the pathogens *Enterococcus faecalis* and *Streptococcus pneumoniae*. We find that the substrate specificity of the two SBDs in the tandem is different, with one SBD preferring asparagine and the other glutamine. Both SBDs can bind glutamine, but the affinities differ by four orders of magnitude, even though the amino acid sequence and tertiary structures are highly conserved. Using a combined structural biology and thermodynamic approach and structure-based engineering, we identified the determinants for substrate affinity of the tandem SBDs of the GlnPQ importers from *L. lactis*, *E. faecalis*, and *S. pneumoniae*.

RESULTS

Gene Organization, Cloning, and Protein Purification

The GlnPQ importers from *L. lactis* (Ll), *E. faecalis* (Ef), and *S. pneumoniae* (Spn) are composed of two subunits: GlnP and GlnQ, and each subunit is utilized twice in the functional transporter complex. GlnP consists of a signal sequence (SQ), two SBDs fused in tandem, and a C-terminal TMD. GlnQ is a typical ABC-type nucleotide-binding protein. Figure S1A (available online) shows the gene organization of the *glnPQ* operon and the neighboring genes in *L. lactis*, *E. faecalis*, and *S. pneumoniae*. Gene *glnP* is followed immediately by *glnQ* and both are expressed from the same promoter. The sequence identity among tandem SBDs of the GlnP proteins from *L. lactis*, *E. faecalis*, and *S. pneumoniae* is approximately 50%, with major differences in the linker region that connects SBD1 and SBD2 (Figure S1B). The residues that interact with the substrate in the crystal structures of SBD1 and SBD2 from *L. lactis* are highlighted in red and are actually well conserved in the other proteins (vide infra).

The genes corresponding to the individual SBDs and the tandem SBD from *E. faecalis, S. pneumoniae*, and *L. lactis* were expressed in *E. coli* (Geertsma et al., 2008). In each case, an N-terminal decahistidine tag followed by the TEV cleavage site preceded the sequence of the mature protein. A two-step purification procedure (immobilized metal affinity chromatography followed by size-exclusion chromatography) typically yielded more than 10 mg of monodisperse protein from 1 l of cell culture (optical density at 600 nm [OD_{600}] ~2.8), both for the individual and tandem SBDs. The purified SBDs were monomeric with a molecular mass of ~25 kDa; the tandem SBDs also behaved as monomeric species (Figure S2).

Substrate Affinity and Specificity

We used isothermal titration calorimetry (ITC) and intrinsic protein fluorescence to characterize the binding of glutamine to the SBD1, SBD2, and SBD12 of GlnPQ from *E. faecalis* and *S. pneumoniae*. ITC is suitable for determining dissociation constants (K_D) in the nanomolar to micromolar range but not for very low affinity binding (submillimolar or higher). In that case, fluorescence measurements can be an alternative, provided the intrinsic protein fluorescence changes upon ligand binding. Contrary to ITC, fluorescence measurements do not provide thermodynamic details (ΔH and $T\Delta S$) of the binding process. SBD1 of GlnP from *S. pneumoniae* ($SBD1_{Spn}$) has two Trp residues that we used to track conformational changes and to determine the K_D of low affinity binding.

The ITC data for glutamine binding to SBD1, SBD2, and SBD12 from *E. faecalis* are presented in Figures 1A–1C, and the data are summarized in Table 1. $SBD1_{Ef}$ binds glutamine with very high affinity (K_D = 0.13 μM); the K_D for glutamine binding to $SBD2_{Ef}$ is 1.5 μM. The binding isotherms of $SBD12_{Ef}$ are a composite of those of $SBD1_{Ef}$ and $SBD2_{Ef}$, but the corresponding K_D values are difficult to resolve. Importantly, the binding isotherm of $SBD12_{Ef}$ is identical to that of a 1-to-1 mixture of $SBD1_{Ef}$ with $SBD2_{Ef}$ (Figures 1C and 1D), indicating that binding of glutamine to one SBD does not influence binding to the other SBD.

The K_D of glutamine binding to SBD1 from *S. pneumoniae* was too high for ITC measurements and was determined with fluorescence titration instead. Glutamine binding led to the decrease of the protein fluorescence, which was used to estimate the K_D of 716 μM (Figure 1E); this value is three orders of magnitude higher than the K_D of 0.7 μM of the corresponding SBD2 (Table 1). We used the same method to test all 20 natural amino acids as potential substrate (Figure S3). Surprisingly, $SBD1_{Spn}$ binds aspartate (K_D = 410 μM) provided the pH is low (pH 3.9 in our measurements), which suggests that aspartic acid rather than aspartate anion is bound. Another remarkable finding is the high-affinity binding of asparagine (K_D = 1.42 μM; Figure 1F) as compared to glutamine (K_D = 716 μM), while the corresponding SBD2 showed low affinity for asparagine and high affinity for glutamine (data summarized in Table 1). The affinity of $SBD2_{Spn}$ toward asparagine was so low that we could not determine the exact K_D value. The K_D values of glutamine binding to SBD1 and SBD2 of GlnPQ from *L. lactis* are 90 and 0.9 μM, respectively (Table 1). $SBD1_{Ll}$ has high affinity for asparagine (K_D = 0.2 μM), whereas we did not detect any interaction between $SBD2_{Ll}$ and asparagine. On the contrary, $SBD2_{Ll}$ does bind glutamic acid, whereas $SBD1_{Ll}$ does not. In summary, we find that the tandem SBDs of GlnPQ transporters from pathogenic and nonpathogenic gram-positive bacteria have evolved differently in terms of substrate specificity and affinity. These functional differences occur not only between GlnPQ transporters from different species, but also between the SBDs of a given polypeptide.

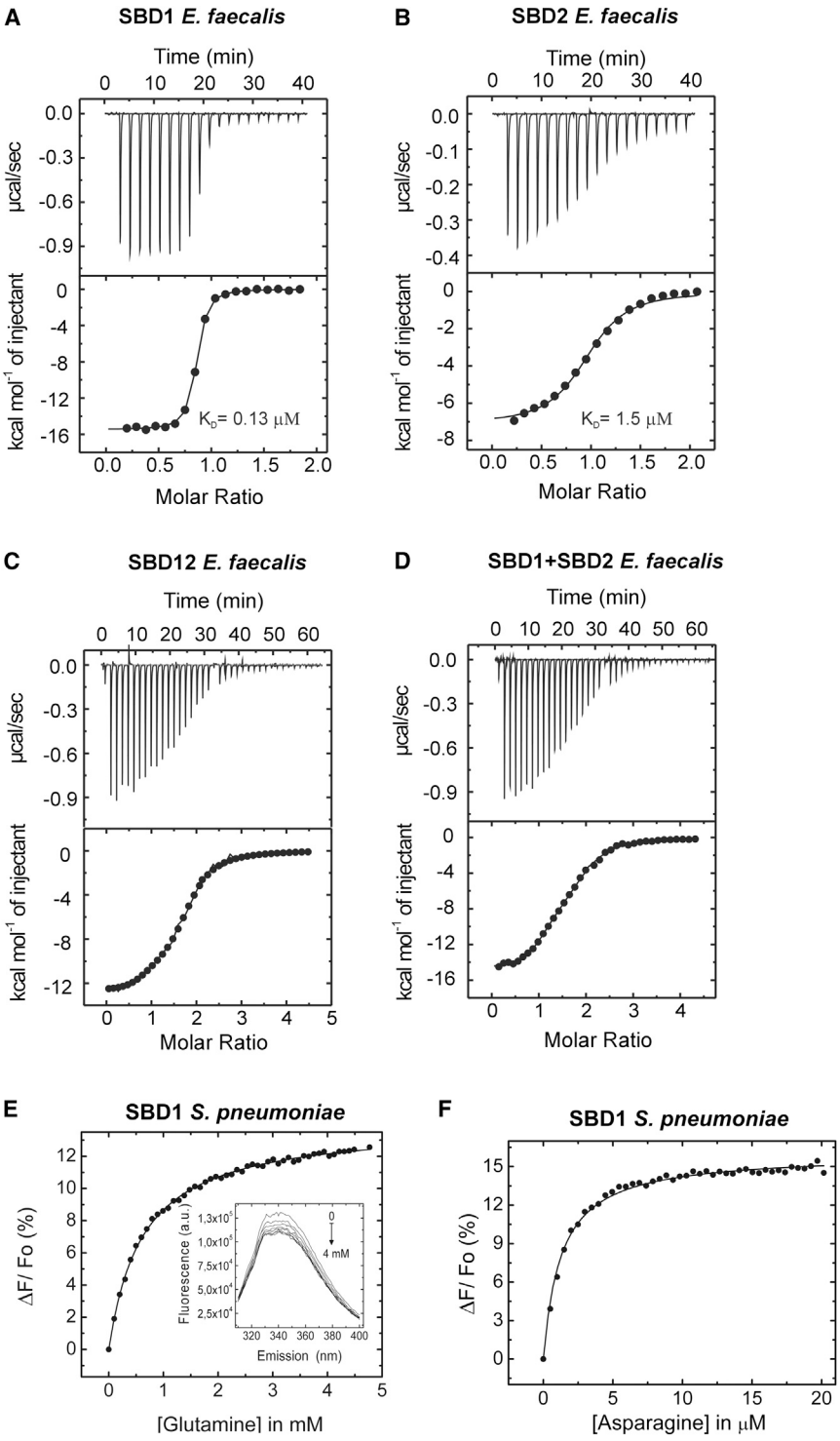

Figure 1. Amino Acid Binding to SBDs of GlnPQ Transporters from *E. faecalis* and *S. pneumoniae*

(A–D) Glutamine binding to SBD1 (A), SBD2 (B), SBD12 (C), and a one-to-one mixture of SBD1 with SBD2 (D) of GlnPQ from *E. faecalis*. ITC measurements were performed in 20 mM Na-Mes at pH 5.5 plus 150 mM NaCl at 298 K. Purified protein at a final concentration of 35–45 µM was used in the experiments. The upper graphs show the heat released by the protein upon glutamine binding, and the area under each injection signal was integrated and plotted in the lower panel. The solid lines in the lower panel represent nonlinear least-squares fits of the reaction heat for the injection. The enthalpy per mole of glutamine injected is plotted as a function of the protein-to-glutamine ratio. In the case of SBD1 plus SBD2, half the concentration in weight (rather than the sum of the concentration of SBD1 plus SBD2) was used to allow for comparison with the SBD12 data.

(E and F) Glutamine and asparagine bind to SBD1 of GlnPQ from *S. pneumonia*, as shown in (E) and (F), respectively. The normalized fluorescence changes at 340 nm were plotted as a function of glutamine (A) and asparagine (B) concentration, yielding K_D values of 716 µM and 1.4 µM, respectively. The emission scans of SBD1 in the absence of glutamine (uppermost trace) and in the presence of successively higher concentrations of glutamine (up to 4 mM) are shown in the inset. The excitation and emission wavelengths were 295 and 340 nm, respectively; the slit widths were 1 and 3 nm. The protein concentration was 1 µM and measurements were done in 100 mM Na-Mes at pH 5.5 plus 150 mM NaCl at 298 K.

See also Figure S3.

Crystallization and Structure Determination

Overall Structures

We solved crystal structures of SBD1 from *L. lactis* and *E. faecalis* and SBD2 from *L. lactis* (summarized in Table 2). The structure of SBD1 of GlnP from *L. lactis* ($SBD1_{Ll}$) was solved in the open-unliganded state at 1.4 Å resolution, whereas structures of $SBD2_{Ll}$ were obtained both in the closed-liganded and open-unliganded states at 0.9 and 1.5 Å resolution, respectively. The structure of SBD1 (244 residues) from *E. faecalis* was solved in a closed-liganded conformation at 1.5 Å resolution. The three SBDs consist of two α/β subdomains: a large one ($SBD1_{Ll}$ residues 29–113, 207–251; $SBD2_{Ll}$ residues 255–345, 441–480; and $SBD1_{Ef}$ residues 1–106 and 207–244) and a small one ($SBD1_{Ll}$ residues 114–206; $SBD2_{Ll}$ residues 346–440; and $SBD1_{Ef}$ residues 111–200). The two domains are connected by two antiparallel β strands, a common feature of class II substrate-binding proteins (Fukami-Kobayashi et al., 1999). In the closed-liganded structures, the substrate glutamine binds in a deep cleft formed by two domains, while the connecting β strands form the base of the cleft. $SBD1_{Ef}$ has an overall structure similar to $SBD2_{Ll}$ with a root-mean-square deviation (rmsd) of 1.0 Å (Figure 2A). According to the recent structural classification of substrate-binding proteins (Berntsson et al., 2010), the GlnPQ SBDs belong

Table 1. Binding Affinity of the SBDs of GlnPQ

Organism (Ligand)	K_D (μM)	ΔH (kJ/mol)	TΔS (kJ/mol)	ΔG (kJ/mol)
E. faecalis (Gln)				
SBD1	0.13 ± 0.01	−67.0 ± 2.5	−28 ± 2.7	−39.1 ± 3.7
SBD2	1.49 ± 0.02	−29.5 ± 0.3	3.8 ± 0.4	−33.3 ± 0.5
SBD1 triple mutant	7.13 ± 0.3	−54.7 ± 1	−25.4 ± 0.9	−29.3 ± 1.3
S. pneumoniae (Gln)				
SBD1	716 ± 126[a]	–	–	–
SBD2	0.7 ± 0.01	−43.9 ± 0.8	−8.8 ± 0.7	−35.1 ± 1.0
SBD1 triple mutant	0.16 ± 0.03	−26 ± 0.9	12.8 ± 0.8	−38.8 ± 1.2
S. pneumoniae (Asn)				
SBD1	1.42 ± 0.1[a]	–	–	–
SBD2	nd	–	–	–
L. lactis (Gln)				
SBD1	92 ± 16	−23.9 ± 6.3	−0.9 ± 0.1	−23.0 ± 7.1
SBD2	0.9 ± 0.2	−19.3 ± 2.2	15.4 ± 0.7	−34.7 ± 2.4
L. lactis (Asn)				
SBD1	0.2 ± 0.0	−73.6 ± 1.2	−34.9 ± 1.1	−38.7 ± 1.6
SBD2	no affinity	–	–	–

Dissociation constants (K_D) and thermodynamic parameters (ΔG, ΔH, and TΔS) of amino acid binding to SBD1 and SBD2 from *E. faecalis*, *S. pneumonia*, and *L. lactis*. nd, not determined due to very low affinity.
[a]Based on intrinsic protein fluorescence measurements.

to Subcluster F-IV, which consists of class II amino acid-binding proteins. DALI searches, using the $SBD2_{LI}$ structure as a query against the Protein Data Bank (PDB), reveals overall highest structural similarity to the *E. coli* glutamine-binding protein GlnBP (PDB code 1WDN), the *Salmonella typhimurium* lysine/arginine/ornithine-binding protein LAO (PDB code 1LAF), the *Geobacillus Stearothermophilus* lysine-binding protein ArtJ (PDB code 2PVU), and the *E. coli* histidine-binding protein HisJ (PDB code 1HSL) with DALI Z-scores of ∼30 for circa 220 aligned Cα atoms. The superposition of $SBD1_{Ef}$ with $SBD1_{LI}$, $SBD2_{LI}$, GlnBP, LAO, HisJ, and ArtJ indeed shows an overall similar fold with rmsd values between 1.0 and 1.6 Å, except for unliganded $SBD1_{LI}$, which gave a rmsd of 3.1 Å (Figure S4).

Comparison of the Open and Closed Conformations

The open-unliganded and closed-liganded structures of $SBD2_{LI}$ show that large structural changes occur upon substrate binding. Both domains move as rigid bodies ∼20° relative to the hinge region made of two β strands connecting subdomains (Figure 2C). Superposition of the small and large subdomains from the $SBD2_{LI}$ open-unliganded and closed-liganded structures does not reveal significant structural changes within the subdomains upon substrate binding (rmsd ∼0.4 Å for the aligned Cα atoms). Glutamine bound to SBD2 is completely buried between the large and the small subdomain. It is predominantly held in place by hydrogen bonds but additionally it makes ionic and hydrophobic interactions, most of which come from the large domain (Figure 2D). Similar interactions were reported for other amino acid-binding SBDs (Oh et al., 1993; Sun et al., 1998; Trakhanov et al., 2005); see subsequent sections.

Glutamine-Binding Site

The SBDs from *L. lactis* have dissociation constants for glutamine of 90 μM (SBD1) and 0.9 μM (SBD2), respectively. To gain insight into the determinants for ligand binding, we compared the structures of these proteins with SBD1 from *E. faecalis*, because $SBD1_{Ef}$ has the highest affinity for glutamine (K_D = 0.13 μM; Table 1). In the closed-liganded state of each protein, L-glutamine is completely buried in a pocket formed between the cleft of the two domains, wherein the large domain provides the majority of interactions with the ligand (Figure 2B). In $SBD1_{EF}$, the α-carboxyl group (COO^-) of the bound glutamine is stabilized by a salt bridge with R96, as well as by hydrogen bonds to the backbone nitrogen atoms of S91 and E140 from the large and small domain, respectively. The α-amino group makes hydrogen bonds with the hydroxyl group of S91, Oδ2 atom of D180, and the backbone carbonyl of G89, all from the large domain. The side chain moiety of the bound glutamine is sandwiched in a hydrophobic pocket formed between F33 and F71. The Nε2 atom of the glutamine forms hydrogen bonds with the Oδ2 atom of D30, and the backbone carbonyl of A88, whereas the glutamine Oε1 atom makes direct hydrogen bonds to Nζ of K136. In addition, the Oε1 atom also makes hydrogen bonds via one and two water molecules with Oδ1 of D179 and the hydroxyl group of S141 side chain, respectively.

In the closed-liganded $SBD2_{LI}$ structure, the binding pocket is the same as that in $SBD1_{Ef}$ with the exception that A88 is replaced by S325 and E140 by A377. These residues, however, provide the same mode of interaction with the glutamine ligand, namely via backbone carbonyl (A88/S325) and backbone nitrogen (E140/A377) atoms. In the $SBD1_{Ef}$ structure, the side chain of E140 is located in the small subdomain, which most likely tightens the closure of the binding pocket by interacting with two residues in the large subdomain, i.e., via a salt bridge with the side chain of R96 and via hydrogen bonding with the hydroxyl group of T93 (Figure S5). These interactions may contribute to the higher affinity of the $SBD1_{Ef}$ for glutamine as compared to the $SBD2_{LI}$ protein.

Comparison of High- and Low-Affinity Ligand-Binding Sites

Similar to the open $SBD2_{LI}$ structure, one of the $SBD1_{LI}$ structures is in an open conformation but with a buffer molecule (MES) bound in the position of glutamine. However, binding of MES does not lead to the closure of domains, because the structure is absolutely identical to the one obtained in MES-free conditions. This indicates that interaction of the amino acid side chain is crucial for substrate recognition. To compare the $SBD1_{LI}$ and $SBD2_{LI}$ ligand-binding sites, we have superimposed separately the small and large subdomains from SBD1 and the closed glutamine-bound SBD2 (rmsds are 1.0 and 0.9 Å for 127 and 96 aligned Cα atoms, respectively; Figure 2D). The two ligand-binding sites are strikingly similar even though their affinities for glutamine differ by two orders of magnitude. Six of the nine amino acid residues from $SBD2_{LI}$ (R333, S328, G326, S325, D267, K373, A377, D416, and D417), directly interacting with the ligand, are strictly conserved in $SBD1_{LI}$. The two nonconserved residues S328 and S325 are replaced by T96 and A93 in $SBD1_{LI}$. The Oγ1 of T96 in $SBD1_{LI}$ is fulfilling the same role as the S328 Oγ atom in $SBD2_{LI}$. The second interaction is provided by the backbone carbonyl to Nε2 atom of the bound glutamine, thus

Table 2. Data Collection and Refinement Statistics

	E. faecalis SBD1 Liganded	*L. lactis* SBD1-MES	*L. lactis* SBD1 Unliganded	*L. lactis* SBD2 Unliganded	*L. lactis* SBD2 Liganded
Data Collection					
Space group	$P2_1$	$P1$	$P1$	$C2$	$P2_1$
Cell Dimensions					
a, b, c (Å)	40.73, 61.14, 45.12	35.10, 55.63, 55.74	35.09, 55.5, 56.01	88.69, 89.12, 59.48	42.99, 51.69, 44.23
α, β, γ (°)	90.00, 99.05, 90.00	93.99, 89.71, 97.98	93.347, 92.924, 97.496	90.00, 95.58, 90.00	90.00, 91.10, 90.00
Resolution range (Å)	44.56–1.5 (1.6–1.5)	17.9–1.4 (1.48–1.4)	34.8–1.4 (1.5–1.4)	19.89–1.5 (1.58–1.5)	44.22–0.95 (1–0.95)
Completeness (%)	97.6 (95.6)	93.6 (92.9)	89.1 (87.5)	98.9 (98.2)	98.5 (95.8)
R_{meas} (%)	4.2 (10.4)	3.0 (29.2)	5.6 (34.0)	4.1 (48.9)	4.7 (45.6)
I/σ (I)	23.8 (14.1)	13.4 (2.5)	6.2 (2.0)	14.3 (1.7)	19.8 (3.2)
Redundancy	3.3 (3.2)	2.0 (2.0)	1.7 (1.7)	2.3 (2.3)	4.2 (3.5)
Refinement					
Resolution range (Å)	36–1.5	17.9–1.4	34.8–1.4	19.89–1.5	44.22–0.95
Number of reflections	34,211	76,731	91,549	72,554	119,814
R_{work}/R_{free} (%)	12.69/15.50	13.95/18.78	15.57/19.45	14.34/18.59	11.47/11.97
No. of atoms					
Protein	1,982	3,520	6,907	3,737	4,009
Ligand (substrate/buffer/PEG/ions)	10/12/–/–	–/–/24/174/–	–/–/49/5	–/–/79/6	20/–/–/–
Water	373	526	627	775	507
Average B-Factors (Å^2)					
Protein	12.9	24.6	23.8	16.0	10.7
Water	25.9	39.3	34.3	27.8	15.2
Ligand (substrate/buffer/PEG)	4.9/22.1/–/–	–/31.0/48.8/–	–/–/44.6/38.3	–/–/38.2/20.1	4.1/–/–/–
Rmsd					
Bond length (Å)	0.008	0.009	0.009	0.009	0.007
Bond angles (°)	1.205	1.245	1.235	1.289	1.281

Values in parentheses are for the highest resolution shell.

this interaction is virtually the same in both structures. The third nonconserved residue in $SBD2_{LI}$ is D417, which is replaced by E184 in $SBD1_{LI}$. The two aromatic residues F270 and F308 harboring the side chain of ligand are conserved in SBD1 as Y38 and F76, respectively. To explain the large differences in affinity of $SBD1_{LI}$ and $SBD2_{LI}$ for glutamine, it seems likely that three nonconserved residues play a role in the full closing of the binding pocket, which may not occur in $SBD1_{LI}$.

Comparison with the Binding Sites of Related Proteins of Subcluster F-IV

The multiple alignment of sequences of $SBD1_{Ef}$, $SBD1_{LI}$, and $SBD2_{LI}$ with several other binding proteins within subcluster F-IV (GlnBP, LAO, ArtJ, and HisJ; Figure S6) revealed 28%–50% identity with $SBD1_{Ef}$. Structural superposition of $SBD1_{Ef}$ and the liganded form of these proteins show that, of 19 conserved residues, the equivalent of R96 and D30 form an electrostatic interaction and hydrogen bond with the ligand, respectively, except for HisJ. In HisJ, the side chain of the corresponding Asp oriented so that the hydrogen bond cannot be formed. Overall, the binding pockets around the α-carboxylate and the α-amino group of the ligand and the arrangement of the hydrogen bond framework are well conserved as also discussed for the glutamate/ aspartate binding protein DEBP (Hu et al., 2008).

On the contrary, the binding pocket for the ligand side chain is poorly conserved, except for the hydrophobic pocket formed by a combination of Phe, Tyr, Trp, or Leu residues that sandwich the side chain moiety of the ligand. The residue A88 (in $SBD1_{Ef}$) is substituted by Ser in $SBD2_{LI}$, HisJ, LAO, and ArtJ. The substitution, however, did not change the interaction mode between the protein and the ligand except in ArtJ. In ArtJ, the hydroxyl group of the corresponding Ser makes water-mediated hydrogen bonds with the Nζ of the lysine ligand (Figure S7A). Replacement of K136 in $SBD1_{Ef}$ with Leu (in HisJ and LAO) abolishes the hydrogen bond interaction with the side chain of the ligand, while in ArtJ, this interaction is conserved through the substitution of Lys with Gln. This Lys residue has been suggested to be important for GlnBP specificity (Sun et al., 1998). Furthermore, the two residues that provide indirect interaction with the ligand in $SBD1_{Ef}$, S141 and D179, are replaced by Ala ($SBD1_{LI}$), Gly (ArtJ), Gln (HisJ, LAO) and His (GlnBP), Thr (ArtJ), and Gln (HisJ, LAO). The substituted residues provide no interaction with the bound ligand except for the substitution of D179 with His (GlnBP), i.e., a hydrogen bond to the Oε1 atom of the glutamine side chain (Figure S7B). These substitutions may tune the affinity for the respective ligand but it is not possible to predict their roles beforehand. We thus set out to engineer the specificity of the

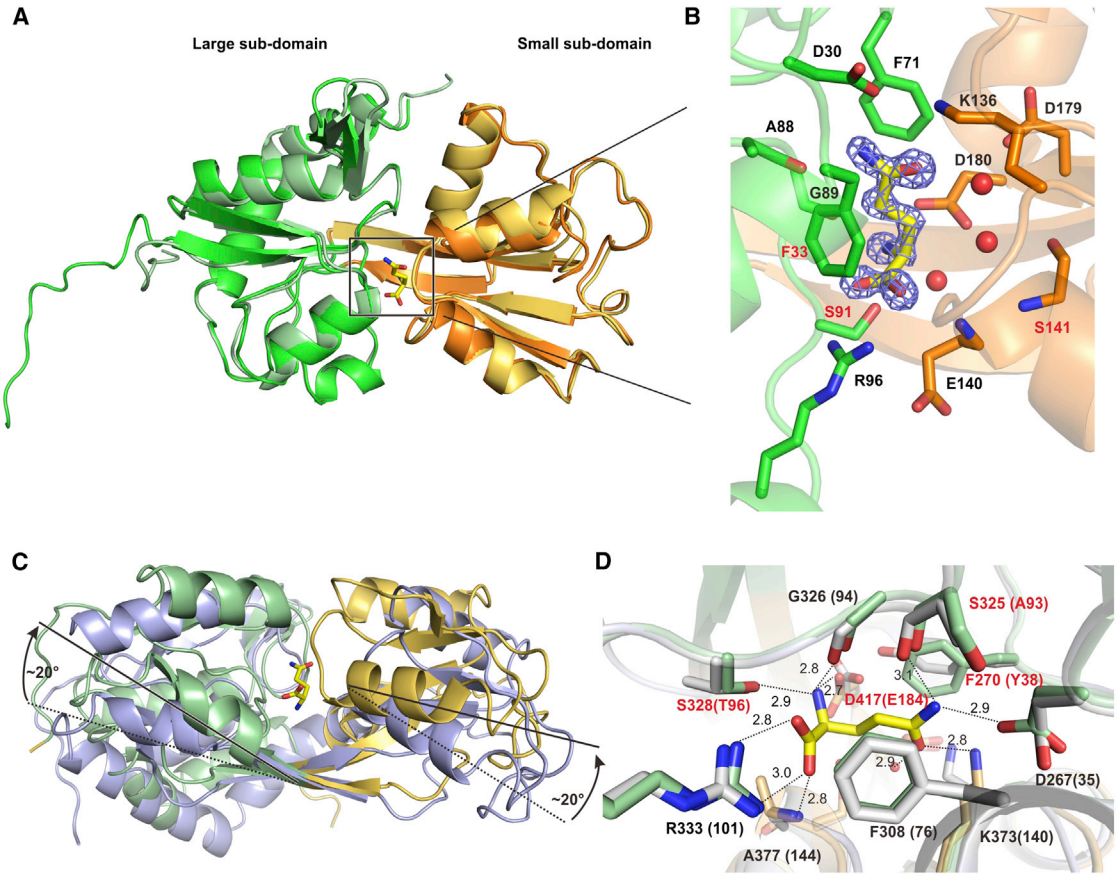

Figure 2. Crystal Structures of SBD1 and SBD2 of GlnPQ from *L. lactis* and *E. faecalis*

(A) Superimposition of crystal structures of closed-liganded SBD1 of GlnPQ from *E. faecalis* solved at 1.5 Å and SBD2 of GlnPQ from *L. lactis* solved at 0.9 Å (rmsd ~1 Å). The large subdomain is colored green ($SBD1_{Ef}$) or pale green ($SBD2_{Ll}$) and the small subdomain is in orange ($SBD1_{Ef}$) or pale orange ($SBD2_{Ll}$). The ligand (glutamine) is shown by stick representation in yellow.

(B) Interactions of bound glutamine with the residues in the binding site of $SBD1_{Ef}$; the coloring of subdomain residues is the same as in (A). Interacting residues are shown as sticks and labeled. Red labels are for key residues, which change SBD's affinity to glutamine. Bound glutamine is colored yellow and the omit F_o-F_c electron density map, contoured at 2.0 σ level, is shown as blue mesh.

(C) Superimposition of unliganded (purple) and liganded (pale green and orange) conformation in $SBD2_{Ll}$. The movements of domains relatively to the hinge region are indicated with black arrows.

(D) Comparison of binding sites of liganded-$SBD2_{Ll}$ (green) and unliganded-$SBD1_{Ll}$ (gray). Nonidentical amino acids are highlighted in red (numbering in parentheses is for SBD1). Distances are given in Ångströms.

See also Figures S2 and S4–S7.

SBDs, taking advantage of the wealth of structural information described heretofore.

Engineering of Binding Affinity

The affinity for glutamine of the SBDs of the GlnPQ ABC transporters from *L. lactis, E. faecalis*, and *S. pneumoniae* varies enormously; the lowest and highest K_D values differ by almost four orders of magnitude (Figure 3). $SBD1_{Ef}$ has the highest affinity and $SBD1_{Spn}$ the lowest affinity. The most notable differences in the binding site residues are highlighted in Figure 3 in orange and green, whereas light blue and blue indicate conserved and highly conserved binding site residues, respectively. The combined data suggest that F33, S91, and S141 are required for high-affinity binding of glutamine in $SBD1_{Ef}$. In the low-affinity $SBD1_{Spn}$, those positions are filled with Y31, T89, and A138. To test this hypothesis, we mutated F33 to Tyr, S91 to Thr, and S141 to Ala in the $SBD1_{Ef}$, which should lead to low-affinity binding by our prediction. Furthermore, we mutated Y31 to Phe, T89 to Ser, and A138 to Ser in the $SBD1_{Spn}$, which should cause the high-affinity binding. Indeed, ITC measurements showed that the K_D for glutamine binding of the $SBD1_{Ef}$ triple mutant was increased from 0.13 to 7.13 μM, whereas the K_D of the $SBD1_{Spn}$ triple mutant was decreased from 720 to 0.16 μM (Figure 4A; Table 1). The high-affinity binding of the $SBD1_{Ef}$ has a large enthalpy term (−67 kJ/mol), which is changed to −54 kJ/mol in the triple mutant, resulting in ~50-fold lower affinity; the entropic term is the same for both proteins. The high-affinity glutamine binding of the $SBD1_{Spn}$ triple mutant has favorable enthalpy and entropy terms, but the ΔH and TΔS term of the parental SBD1 could not be determined. The $SBD1_{Spn}$ triple mutant still binds asparagine with relatively high affinity.

L. lactis		*E. faecalis*		*S. pneumoniae*	
SBD1	SBD2	SBD1	SBD2	SBD1	SBD2
D35	D267	D30	D273	D28	D271
Y38	F270	F33	F276	Y31	F274
F76	F308	F71	F314	F69	F312
A93	S325	A88	A331	A86	A329
G94	G326	G89	G332	G87	G330
T96	S328	S91	T334	T89	S332
R101	R333	R96	R339	R94	R337
K140	K373	K136	K379	K133	K376
A144	A377	E140	E383	A137	A380
A145	S378	S141	S384	A138	S381
D183	D416	D179	D422	D176	D419
E184	D417	D180	D423	D177	D420
90 μM	0.9 μM	0.13 μM	1.49 μM	716 μM	0.71 μM

Figure 3. Comparison of Amino Acid Binding Sites in SBDs from Nonpathogenic and Pathogenic Bacteria

The glutamine-binding sites of the SBD1 and SBD2 of the GlnPQ transporters from *L. lactis, E. faecalis*, and *S. pneumonia* are shown. The residues indicated are those that interact with the substrate. The most notable differences in the binding site residues are highlighted in orange and green, whereas light blue and blue indicate conserved and highly conserved binding site residues, respectively. The dissociation constants for glutamine of each of the proteins are indicated in the bottom line. See also Figure S1.

The observation that the affinity of the $SBD1_{Spn}$ for glutamine can be increased by four orders of magnitude by introducing only three conservative substitutions is remarkable. This prompted us to investigate the contribution of the individual amino acid substitutions. To perform that, we used the tryptophan fluorescence measurement technique, because the K_D values were too high for ITC. Figure 4B shows that the single mutants have dissociations constants for glutamine in the range from 40 to 150 μM, which is about an order of magnitude smaller than that of the wild-type $SBD1_{Spn}$ and two orders of magnitude higher than that of the triple mutant. This result demonstrates that each of the residues contributes directly to the binding affinity.

DISCUSSION

The crystal structures of 25 homologs of the *L. lactis, E. faecalis*, and *S. pneumoniae* GlnPQ SBDs have been deposited in the PDB; biochemical data on substrate binding are available for some of these proteins (summarized in Table S1). However, the SBPs of known structures are either periplasmic (gram-negative bacteria) or lipid-tethered proteins, in contrast to the aforementioned transporters where two SBDs are fused in tandem and linked to the TMD. Importantly, despite the wealth of structural data and observations that SBPs bind their ligands with nanomolar to submillimolar affinity, little is known of the actual affinity and specificity determinants. In addition to the ABC transporter-linked SBDs, a number of crystal structures are available of homologous receptors, which are associated with ionotropic glutamate receptors (Jin et al., 2009; O'Hara et al., 1993). We now show that ABC transporter-linked SBDs with almost identical overall folds and similar binding pockets can bind glutamine with affinities that differ by more than four orders of magnitude. Furthermore, we reveal that dual substrate specificity of the ABC transporters can be achieved with the tandem-linked SBDs. The *S. pneumoniae* and *L. lactis* GlnPQ use one of the SBDs to bind glutamine with high affinity and asparagine with low affinity and the other SBD having a reciprocal specificity, allowing different amino acids to be accumulated via the same transporter. Some SBDs also bind glutamic acid or aspartic acid but not the anionic form of these amino acids, which requires a low pH or they will otherwise be outcompeted by glutamine and/or asparagine.

In ABC transporters with soluble, periplasmic substrate-binding proteins, the transmembrane domain usually interacts with a single receptor (Davidson et al., 2008), but there are exceptions. In the histidine transporter from *Salmonella typhimurium,* the transmembrane domain interacts with two different substrate-binding proteins (HisJ and ArgT), allowing a greater diversity of substrates to be taken up (Higgins and Ames, 1981). This is analogous to ABC transporters with tandem-linked domains. Because the affinity of type I ABC importers for liganded SBDs is low (about 50 μM; Dean et al., 1992; Doeven et al., 2004; Prossnitz et al., 1989), the SBD concentration at the site of translocation matters. By linking the SBDs to the TMD, the transporter ensures a high local concentration and thus efficient transport. In the GlnPQ systems, the efficient transport is combined with a broader substrate specificity and a combination of high- and low-affinity sites within the same system. For example, SBD1 from *S. pneumoniae* showed a preference for asparagine (K_D = 1.4 μM) compared to glutamine (K_D = 716 μM), while the corresponding SBD2 showed the opposite selectivity (Table 1). Similarly, SBD1 from *L. lactis* binds asparagine with high affinity (K_D = 0.2 μM) and glutamine with low affinity (K_D = 92 μM), whereas SBD2 only accepts glutamine (and glutamic acid). It is possible that the high-affinity site allows the scavenging of amino acids when nutrient conditions are limited, whereas the low-affinity site allows for faster transport when amino acids are available in excess (Lanfermeijer et al., 1999). In this way, the GlnPQ transporters combine several properties that allow the uptake of different amino acids that are needed at high concentrations in the cell, under conditions of varying nutrient availability.

Biologic activity of a molecule is driven by free energy changes with enthalpic (static interactions) and entropic (dynamic interactions) contributions. The ITC data on the binding of glutamine to wild-type and mutant $SBD1_{Ef}$ indicate that the negative ΔH term is the determinant for high-affinity ligand binding. Compared to the $SBD2_{Ef}$, the $SBD1_{Ef}$ has a more favorable (more negative) ΔH and less favorable (more positive) TΔS. Our structural analysis shows that the binding sites for amino acids in the different SBD1 and SBD2 proteins are similar and from the structures alone, it is not evident what determines the specificity and/or ligand affinity. It is possible that low-affinity ligands are unable to fully close the binding site and thus form fewer interactions with the protein than high-affinity ligands. In the case of glutamine, the extra methylene group could render the ligand too bulky, thus preventing full closure of the binding pocket of $SBD1_{Ll}$, which would in turn result in a lower affinity. In the case of $SBD2_{Ll}$, the closed binding pocket may be larger,

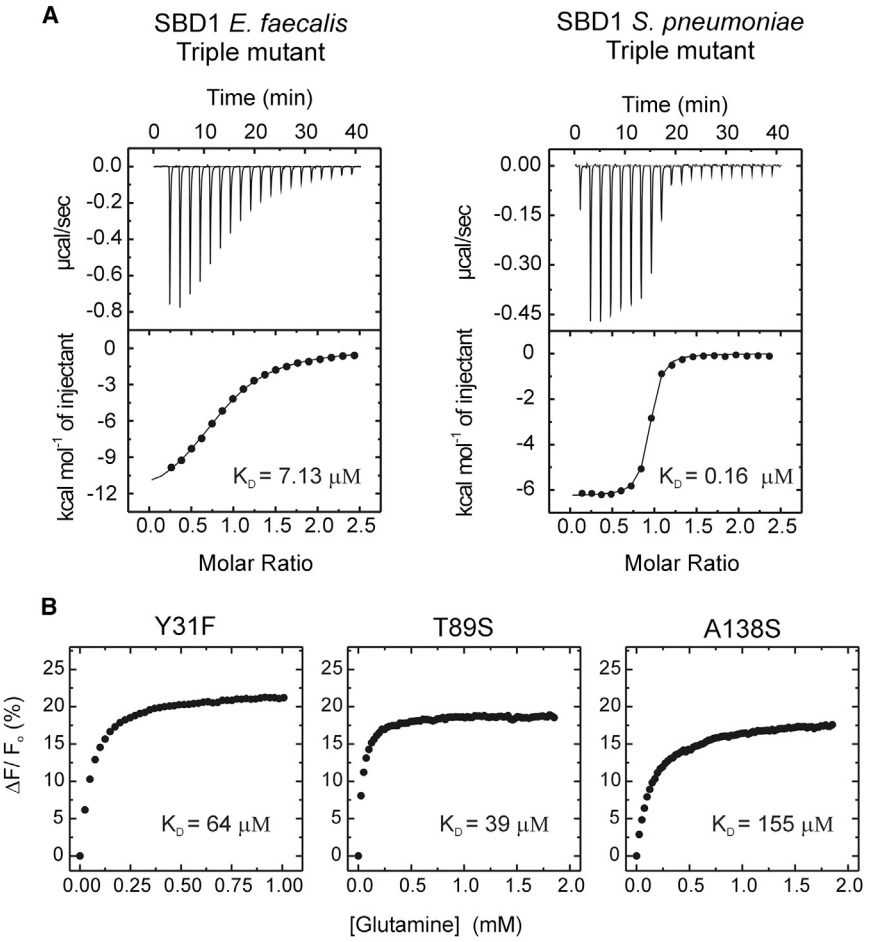

Figure 4. Glutamine Binding to Engineered SBDs

(A) Glutamine binding to the *E. faecalis* and *S. pneumoniae* SBD1 triple mutants as determined with ITC. The experimental conditions were the same as those described in Figure 1.

(B) Glutamine binding to the *S. pneumoniae* SBD1 single mutants (mutations are denoted above the subpanels) as determined with intrinsic protein fluorescence measurements.

allowing more interactions between the protein and glutamine than between the protein and asparagine. Here, one could speculate that too few interactions between asparagine and the protein preclude full closure of the binding pocket. In fact, we have preliminary single-molecule FRET data that point to a correlation between the extent of SBD closure and high-affinity binding.

Protein-ligand interactions are determined by hydrogen bonding and electrostatic, electron-π, hydrophobic, and van der Waals interactions between a protein and its substrate. In the case of $SBD1_{Ef}$, eight direct hydrogen bonds between side chain/backbone residues and glutamine are present. In addition, salt bridges and electron-π interactions contribute to the binding. However, it is also known that conformational entropy, i.e., internal dynamics, contributes to the protein-ligand interactions and thus to protein activity and binding affinity (Tzeng and Kalodimos, 2012). Slow internal motions, related to poorly populated conformational states, can affect activity in a manner that is not readily predicted from static X-ray structures. Our mutational analysis of high- and low-affinity SBDs suggests that differences in the binding of glutamine are largely due to differences in amino acids in the binding pocket rather than second-shell residues or long-range effects. Remarkably, the amino acid substitutions that lead to large changes in the binding affinity are all conservative, and the effects are not readily predicted from the sequences. A similar property has been described for the glycine betaine/proline binding protein from *Archaeoglobus fulgidus*; here, a single mutation in the binding site enhanced binding affinity by four orders of magnitude (Tschapek et al., 2011).

For *L. lactis*, a nonpathogenic gram-positive bacterium related to *E. faecalis* and *S. pneumoniae*, the GlnPQ transporter is essential for growth in amino acid-containing media. *L. lactis* as well as many gram-positive pathogens require glutamine or glutamate for biosynthesis and osmoregulation. Accumulated glutamine is readily converted into glutamate and the latter is generally the most abundant amino acid in the bacterial cytoplasm (Poolman et al., 1987). All these requirements warrant an efficient transport of glutamine and glutamate. In *B. streptococci,* GlnPQ plays a role in virulence by affecting the regulation of expression of fibronectin adhesion (Tamura et al., 2002). Deletion of the glutamine transporters SPD 1098/1099 in *S. pneumoniae* D39 (equivalent gene to SP1241/1242 in *S. pneumoniae* TIGR4) diminished bacterial fitness and virulence (Härtel et al., 2011). Moreover, mutations on *glnP* from *S. pneumoniae* significantly reduced the adhesion ability of the bacterium to human pharyngeal epithelial cell, suggesting an important role of the GlnPQ ABC transporter in host colonization (Kloosterman et al., 2006). The natural auxotrophy for Gln/Glu and the requirement for GlnPQ to take up these amino acids makes this transporter a promising target for drug/antibiotic development. Finding an effector of the SBDs that abolishes transport would make the compound effective without the need to enter the cell. Currently, we are exploring the structures of the GlnPQ domains to design and test small molecule inhibitors of glutamine and glutamate transport.

In conclusion, we show that tandem SBDs allow single ABC transporters to capture different amino acids with high and low affinity, making the process flexible and efficient. We have engineered the specificity determinants of the ABC transporters and show that a few conservative substitutions in the active site of the SBDs can increase the substrate affinity by three to four orders of magnitude. Because the binding sites have a very similar architecture, the molecular determinants of high-affinity binding are most probably valid for SBDs of other ABC transporters from subcluster F-IV. The point mutations in the same

architecture of binding sites, coupled with small, yet sufficiently different ligand size, suggest control of SBD closure and provide an elegant way to use the same transporter for uptake of several amino acids. The ability to discriminate glutamine (and glutamic acid) from asparagine by nearly the same SBDs allows the efficient transport without direct competition. It is likely that dual specificity and affinity is a general feature of other subfamilies of ABC transporters, for which our study may serve as starting point for further investigations.

EXPERIMENTAL PROCEDURES

Miscellaneous

The genes coding for the GlnPQ-derived SBDs were amplified with PCR from genomic DNA of *E. faecalis* V583, *S. pneumoniae* TIGR4, and *L. lactis* IL1403 and nLIC complementary primers (Geertsma and Poolman, 2007). The first 23–28 amino acids corresponding to the signal sequence were omitted. The construction of plasmids, the crystallization of the proteins, and the structure determination are described in the Supplemental Experimental Procedures.

Overexpression of GlnPQ-Derived Substrate-Binding Domains

E. coli MC1061, expressing wild-type or mutant variants of GlnPQ-SBDs, was cultivated aerobically in Luria Broth medium supplemented with 1% (w/v) glucose plus 10 μg/ml ampicillin at 37°C. The cells were induced using 2 × 10^{-3}% (w/v) L-arabinose at an OD_{600} ~0.5 and growth was continued for 2 more hours. Cells were harvested by centrifugation 10,000 × *g* for 30 min at 4°C, washed once, and resuspended in 50 mM potassium phosphate (KPi) at pH 7.0 plus 150 mM NaCl (buffer A), and stored at −80°C.

Protein Purification

The frozen cells were thawed at room temperature and diluted to an OD_{600} of ~100 with buffer A. Subsequently, 100 μg/ml deoxyribonuclease type I, 10 mM $MgSO_4$, plus 0.1 mM phenylmethanesulfonyl fluoride (PMSF) were added. The cells were broken by a single pass in a cell disruptor at 25,000 psi and 5°C (Constant System). The cell lysate was mixed with 5 mM Na-EDTA to prevent protein degradation. The unbroken cells and cell debris were removed by ultracentrifugation at 267,000 × *g* for 90 min at 4°C. The supernatant was collected and 0.5 ml Nickel-Sepharose resin (Amersham Biosciences) was added per 10 ml cell lysate. The mixture was incubated for 1 hr at 4°C in 50 mM KPi at pH 8, 200 mM KCl, plus 10% (v/v) glycerol (buffer B) supplemented with 20 mM imidazole. Subsequently, the resin was poured into a 10 ml disposable column (BioRad) and washed with 20 column volumes (CV) of buffer B containing 50 mM imidazole. The protein was eluted in three fractions of one CV, using buffer B supplemented with 500 mM imidazole. The second elution fraction (containing most of the purified protein) was loaded onto a Superdex 200 gel filtration column (GE Healthcare) equilibrated with buffer C (20 mM Na-Mes at pH 5.5 and 150 mM NaCl). Fractions containing SBD protein were collected and concentrated to ~20 mg/ml, using Vivaspin 30 or 50 kDa molecular weight cutoff (MWCO). For the binding experiment, an additional step was used before eluting the protein. The potentially bound ligands were removed by partial unfolding of the protein while bound to the Ni-Sepharose resin, followed by refolding (Staiano et al., 2005; Vahedi-Faridi et al., 2008). The following wash steps were performed consecutively to partially unfold-refold the protein: 40 CV of 2 M guanidine-HCl (GndHCl), 4 CV of 1.5 M GndHCl, 4 CV of 1 M GndHCl, 4 CV of 0.5 M GndHCl, and finally 8 CV of 0 M GndHCl (all in buffer B as basal solvent).

For SBDs of GlnPQ from *L. lactis*, the His-tag was cleaved off by His-tagged-TEV protease at a ratio of 1:40 (w/w) with respect to the purified protein; subsequently, the protein was dialyzed against 50 mM Tris-HCl at pH 8.0, 0.5 mM EDTA, plus 0.5 mM dithiothreitol overnight at 4°C. The His-tagged TEV and residual uncut protein were removed using 0.5 ml bed volume of Ni^{2+}-sepharose. The flow-through of the column was concentrated with a Vivaspin concentrator (GE Healthcare) with a 10 kDa cutoff. Concentrated protein was loaded to a Superdex-200 column (GE Healthcare) and eluted with 20 mM HEPES-NaOH at pH 7.5 plus 150 mM NaCl. Crystallization trials were set up immediately after purification, whereas for other purposes the proteins were stored at −80°C after flash-freezing in liquid N_2.

Isothermal Titration Calorimetry

ITC experiments were conducted using the ultrasensitive ITC200 calorimeter (MicroCal) at 25°C. Glutamine in buffer C (approximately 40 μl) at a concentration of 350–500 μM was added stepwise into the temperature-equilibrated ITC cell filled with ~200 μl of SBD protein in the same buffer and at a concentration of 35–50 μM. The experiments were repeated at least three times. Control measurements included titration of buffer C into the protein solution. For *L. lactis*, SBD's measurements were performed after overnight dialysis against 50 mM KPi at pH 6.0, 1 mM EDTA and 1 mM NaN_3, using substrate solutions prepared in dialysis buffer.

Data were analyzed by using the nonlinear curve-fitting functions for one binding site (Wiseman et al., 1989), provided by the ORIGIN-based software of MicroCal. The calculated curve was obtained from the best-fitting parameters and was used to determine the molar enthalpy change for protein-ligand complex formation, stoichiometry (n), and the corresponding association constant (K_A). The dissociation constant (K_D) is defined as $1/K_A$, and the standard free energy change of binding, $\Delta G = -$ RT ln(K_A). The molar entropy change, ΔS, was calculated from $\Delta G = \Delta H - T\Delta S$.

Fluorescence Spectroscopy

Substrate binding was measured on a Spex Fluorolog 322 fluorescence spectrophotometer (Jobin Yvon) in a stirred quartz cuvette at 25°C. Purified SBD1 from *S. pneumoniae* was diluted in buffer 100 mM Mes at pH 5.5 plus 150 ml NaCl to a concentration of 1 μM (final volume 1 ml) and incubated for 5 min under mild stirring to reach the equilibration temperature before stepwise addition of the substrate (or buffer as control). In the aspartate binding experiment, the buffer was changed to 50 mM Na-acetate pH 3.9 plus 150 mM NaCl. The substrate was added in 1 μl steps, using a pump (Harvard apparatus) fitted with a 500 μl gastight glass syringe (Hamilton). The syringe was connected to the cuvette by tubing with an internal diameter of 0.13 mm (Vici AG International). The excitation wavelength was 295 nm and the emission was measured at 340 nm with the slit width at 1 and 3 nm, respectively. The signal was measured for 20 s following 5 s of mixing time to ensure full equilibration. Fluorescence titrations were analyzed as described previously (Lanfermeijer et al., 1999), and curve fitting was performed with ORIGIN software.

SUPPLEMENTAL INFORMATION

Supplemental Information includes Supplemental Experimental Procedures, seven figures, and one table and can be found with this article online at http://dx.doi.org/10.1016/j.str.2013.07.020.

ACKNOWLEDGMENTS

This work was supported by grants from the Netherlands Organization for Scientific Research (NWO, Top-subsidy grant 700.56.302 to B.P. and a Vici grant to D.-J.S.) and the EU (EDICT program). The authors are grateful to the beam line personnel at 14-1, ID 23-1 (ESRF, Grenoble) and X06SA (SLS, Villigen) for technical assistance.

Received: May 3, 2013
Revised: July 5, 2013
Accepted: July 23, 2013
Published: August 29, 2013

REFERENCES

Bao, H., and Duong, F. (2013). ATP alone triggers the outward facing conformation of the maltose ATP-binding cassette transporter. J. Biol. Chem. *288*, 3439–3448.

Berger, E.A., and Heppel, L.A. (1974). Different mechanisms of energy coupling for the shock-sensitive and shock-resistant amino acid permeases of *Escherichia coli*. J. Biol. Chem. *249*, 7747–7755.

Berntsson, R.P., Smits, S.H., Schmitt, L., Slotboom, D.J., and Poolman, B. (2010). A structural classification of substrate-binding proteins. FEBS Lett. *584*, 2606–2617.

Böhm, S., Licht, A., Wuttge, S., Schneider, E., and Bordignon, E. (2013). Conformational plasticity of the type I maltose ABC importer. Proc. Natl. Acad. Sci. USA *110*, 5492–5497.

Davidson, A.L., Dassa, E., Orelle, C., and Chen, J. (2008). Structure, function, and evolution of bacterial ATP-binding cassette systems. Microbiol. Mol. Biol. Rev. *72*, 317–364.

Dean, D.A., Hor, L.I., Shuman, H.A., and Nikaido, H. (1992). Interaction between maltose-binding protein and the membrane-associated maltose transporter complex in Escherichia coli. Mol. Microbiol. *6*, 2033–2040.

Doeven, M.K., Abele, R., Tampé, R., and Poolman, B. (2004). The binding specificity of OppA determines the selectivity of the oligopeptide ATP-binding cassette transporter. J. Biol. Chem. *279*, 32301–32307.

Erkens, G.B., Berntsson, R.P., Fulyani, F., Majsnerowska, M., Vujičić-Žagar, A., Ter Beek, J., Poolman, B., and Slotboom, D.J. (2011). The structural basis of modularity in ECF-type ABC transporters. Nat. Struct. Mol. Biol. *18*, 755–760.

Erkens, G.B., Majsnerowska, M., ter Beek, J., and Slotboom, D.J. (2012). Energy coupling factor-type ABC transporters for vitamin uptake in prokaryotes. Biochemistry *51*, 4390–4396.

Fukami-Kobayashi, K., Tateno, Y., and Nishikawa, K. (1999). Domain dislocation: a change of core structure in periplasmic binding proteins in their evolutionary history. J. Mol. Biol. *286*, 279–290.

Geertsma, E.R., and Poolman, B. (2007). High-throughput cloning and expression in recalcitrant bacteria. Nat. Methods *4*, 705–707.

Geertsma, E.R., Groeneveld, M., Slotboom, D.J., and Poolman, B. (2008). Quality control of overexpressed membrane proteins. Proc. Natl. Acad. Sci. USA *105*, 5722–5727.

Härtel, T., Klein, M., Koedel, U., Rohde, M., Petruschka, L., and Hammerschmidt, S. (2011). Impact of glutamine transporters on pneumococcal fitness under infection-related conditions. Infect. Immun. *79*, 44–58.

Higgins, C.F., and Ames, G.F. (1981). Two periplasmic transport proteins which interact with a common membrane receptor show extensive homology: complete nucleotide sequences. Proc. Natl. Acad. Sci. USA *78*, 6038–6042.

Hu, Y., Fan, C.P., Fu, G., Zhu, D., Jin, Q., and Wang, D.C. (2008). Crystal structure of a glutamate/aspartate binding protein complexed with a glutamate molecule: structural basis of ligand specificity at atomic resolution. J. Mol. Biol. *382*, 99–111.

Jin, R., Singh, S.K., Gu, S., Furukawa, H., Sobolevsky, A.I., Zhou, J., Jin, Y., and Gouaux, E. (2009). Crystal structure and association behaviour of the GluR2 amino-terminal domain. EMBO J. *28*, 1812–1823.

Joseph, B., Jeschke, G., Goetz, B.A., Locher, K.P., and Bordignon, E. (2011). Transmembrane gate movements in the type II ATP-binding cassette (ABC) importer BtuCD-F during nucleotide cycle. J. Biol. Chem. *286*, 41008–41017.

Kloosterman, T.G., Hendriksen, W.T., Bijlsma, J.J., Bootsma, H.J., van Hijum, S.A., Kok, J., Hermans, P.W., and Kuipers, O.P. (2006). Regulation of glutamine and glutamate metabolism by GlnR and GlnA in *Streptococcus pneumoniae*. J. Biol. Chem. *281*, 25097–25109.

Korkhov, V.M., Mireku, S.A., and Locher, K.P. (2012). Structure of AMP-PNP-bound vitamin B12 transporter BtuCD-F. Nature *490*, 367–372.

Lanfermeijer, F.C., Picon, A., Konings, W.N., and Poolman, B. (1999). Kinetics and consequences of binding of nona- and dodecapeptides to the oligopeptide binding protein (OppA) of *Lactococcus lactis*. Biochemistry (N. Y.) *38*, 14440–14450.

Oh, B.H., Pandit, J., Kang, C.H., Nikaido, K., Gokcen, S., Ames, G.F., and Kim, S.H. (1993). Three-dimensional structures of the periplasmic lysine/arginine/ornithine-binding protein with and without a ligand. J. Biol. Chem. *268*, 11348–11355.

O'Hara, P.J., Sheppard, P.O., Thøgersen, H., Venezia, D., Haldeman, B.A., McGrane, V., Houamed, K.M., Thomsen, C., Gilbert, T.L., and Mulvihill, E.R. (1993). The ligand-binding domain in metabotropic glutamate receptors is related to bacterial periplasmic binding proteins. Neuron *11*, 41–52.

Oldham, M.L., and Chen, J. (2011). Crystal structure of the maltose transporter in a pretranslocation intermediate state. Science *332*, 1202–1205.

Orelle, C., Ayvaz, T., Everly, R.M., Klug, C.S., and Davidson, A.L. (2008). Both maltose-binding protein and ATP are required for nucleotide-binding domain closure in the intact maltose ABC transporter. Proc. Natl. Acad. Sci. USA *105*, 12837–12842.

Poolman, B., Smid, E.J., Veldkamp, H., and Konings, W.N. (1987). Bioenergetic consequences of lactose starvation for continuously cultured Streptococcus cremoris. J. Bacteriol. *169*, 1460–1468.

Prossnitz, E., Gee, A., and Ames, G.F. (1989). Reconstitution of the histidine periplasmic transport system in membrane vesicles. Energy coupling and interaction between the binding protein and the membrane complex. J. Biol. Chem. *264*, 5006–5014.

Rees, D.C., Johnson, E., and Lewinson, O. (2009). ABC transporters: the power to change. Nat. Rev. Mol. Cell Biol. *10*, 218–227.

Rice, A.J., Alvarez, F.J., Schultz, K.M., Klug, C.S., Davidson, A.L., and Pinkett, H.W. (2013). EPR spectroscopy of $MolB_2C_2$-A reveals mechanism of transport for a bacterial type II molybdate importer. J. Biol. Chem. *288*, 21228–21235.

Rodionov, D.A., Hebbeln, P., Eudes, A., ter Beek, J., Rodionova, I.A., Erkens, G.B., Slotboom, D.J., Gelfand, M.S., Osterman, A.L., Hanson, A.D., and Eitinger, T. (2009). A novel class of modular transporters for vitamins in prokaryotes. J. Bacteriol. *191*, 42–51.

Staiano, M., Scognamiglio, V., Rossi, M., D'Auria, S., Stepanenko, O.V., Kuznetsova, I.M., and Turoverov, K.K. (2005). Unfolding and refolding of the glutamine-binding protein from *Escherichia coli* and its complex with glutamine induced by guanidine hydrochloride. Biochemistry *44*, 5625–5633.

Sun, Y.J., Rose, J., Wang, B.C., and Hsiao, C.D. (1998). The structure of glutamine-binding protein complexed with glutamine at 1.94 A resolution: comparisons with other amino acid binding proteins. J. Mol. Biol. *278*, 219–229.

Tamura, G.S., Nittayajarn, A., and Schoentag, D.L. (2002). A glutamine transport gene, glnQ, is required for fibronectin adherence and virulence of group B streptococci. Infect. Immun. *70*, 2877–2885.

Trakhanov, S., Vyas, N.K., Luecke, H., Kristensen, D.M., Ma, J., and Quiocho, F.A. (2005). Ligand-free and -bound structures of the binding protein (LivJ) of the Escherichia coli ABC leucine/isoleucine/valine transport system: trajectory and dynamics of the interdomain rotation and ligand specificity. Biochemistry *44*, 6597–6608.

Tschapek, B., Pittelkow, M., Sohn-Bösser, L., Holtmann, G., Smits, S.H., Gohlke, H., Bremer, E., and Schmitt, L. (2011). Arg149 is involved in switching the low affinity, open state of the binding protein AfProX into its high affinity, closed state. J. Mol. Biol. *411*, 36–52.

Tzeng, S.R., and Kalodimos, C.G. (2012). Protein activity regulation by conformational entropy. Nature *488*, 236–240.

Vahedi-Faridi, A., Eckey, V., Scheffel, F., Alings, C., Landmesser, H., Schneider, E., and Saenger, W. (2008). Crystal structures and mutational analysis of the arginine-, lysine-, histidine-binding protein ArtJ from *Geobacillus stearothermophilus*. Implications for interactions of ArtJ with its cognate ATP-binding cassette transporter, Art(MP)2. J. Mol. Biol. *375*, 448–459.

van der Heide, T., and Poolman, B. (2002). ABC transporters: one, two or four extracytoplasmic substrate-binding sites? EMBO Rep. *3*, 938–943.

Wiseman, T., Williston, S., Brandts, J.F., and Lin, L.N. (1989). Rapid measurement of binding constants and heats of binding using a new titration calorimeter. Anal. Biochem. *179*, 131–137.

